Energy Conversion and Management 105 (2015) 93–102

Contents lists available at ScienceDirect

Energy Conversion and Management

journal homepage: www.elsevier.com/locate/enconman

Comprehensive parametric study of using carbon foam structures saturated with PCMs in thermal management of electronic systems

S.A. Nada *, W.G. Alshaer

Department of Mechanical Engineering, Benha Faculty of Engineering, Benha University, Benha, Egypt

ARTICLE INFO

Article history:
Received 13 May 2015
Accepted 25 July 2015

Keywords:
Parametric study
Carbon foam
PCM
Thermal management
Electronic system

ABSTRACT

The focus of the present work is to perform detailed parametric studies for electronic thermal management systems using different carbon foam structures of different porosities and skeleton thermal conductivities saturated with different phase change materials (PCMs) of different fusion temperatures, heat of fusions and thermal conductivities. Different thicknesses of thermal management modules and power densities levels are also included in the parametric study. The analysis was carried out using a validated finite element numerical model based on volume averaging technique and single-domain energy equation. The results show that decreasing CF and PCM thermal conductivities, increasing carbon foam porosity and increasing module height increase the module temperature and delay the approaching steady state temperature. The transient module temperature decreased and the time of approaching steady state temperature is delayed with increasing PCM heat of fusion. However the module fusion temperature does not show any strong effect on module temperature. Design guidelines for selecting the combinations of CF/PCM thermo-physical properties are presented for different operating conditions and power levels.

1. Introduction

Thermal energy storage and management systems using phase change materials (PCMs) have been widely considered as effective techniques of energy storage systems and thermal management of various engineering applications especially in solar energy applications and electronic equipment applications, respectively. Latent heat thermal energy storage units of PCMs are widely considered due to their high energy storage density and isothermal behavior during the heat storing and retrieving processes. For comprehensive details of using various PCMs in thermal management systems and other engineering applications we refer to the recent review articles [1–7]. Farid et al. [1] presented a detailed review on PCMs, encapsulation and various applications of phase change energy storage systems. Verma et al. [2] reviewed the mathematical modeling of the latent heat storage system using PCMs, by differentiating the models based on first and second law of thermodynamics. Agyenim et al. [3] presented a detailed review on PCMs for the last three decades investigating heat transfer, enhancement techniques and phase change formulation for latent heat thermal energy storage system. Mallik et al. [7] reviewed the state-of-the-art in thermal management materials which may be applicable to an automotive electronic control unit (ECU). This review showed that within the different materials currently available, the Al/SiC composites in particular had very good potential for ECU application.

The major drawback in the PCM based latent heat storage system is its low thermal conductivity, which offers greater resistance to heat transfer rate. To overcome this, several techniques for the enhancement of the thermal conductivity of the PCM, such as providing internal fins and carbon fibers inside the PCM containers, or mixing of high thermal conductivity nanoparticles with the PCM in suspension are studied by several researchers. Hussein et al. [8] used metal screens placed inside the PCMs to improve PCM thermal conductivity. Wang et al. [9] conducted transient three-dimensional heat transfer numerical simulations to investigate a hybrid PCM-based multi-fin heat sink. The study showed that the operating temperature can be controlled well by the attendance of phase change material. They also reported that longer melting time can be conducted by using a multi-fin hybrid heat sink. Hoogendoorn and Bart [10] and Zhang et al. [11] demonstrated the effect of imbedding metal matrices such as metallic foam and metallic sponge in PCM. They reported that the low thermal conductivity of the PCMs can be greatly enhanced by embedding PCM within a metal matrix structure. More recently, Parrado

* Corresponding author. Mobile: +20 1066611381.
E-mail address: samehnadar@yahoo.com (S.A. Nada).

http://dx.doi.org/10.1016/j.enconman.2015.07.071
0196-8904/

Nomenculture

$corr$	correction factor, dimensionless
c_p	specific heat (J/kg K)
g_l	liquid fraction of the fluid phase, dimensionless
h_L	liquid phase enthalpy (J/kg)
k_{eff}	effective thermal conductivity (W/m K)
L	latent heat (J/kg)
T	temperature (K)
T_{onset}	PCM melting onset temperature (K)
T_{endset}	PCM melting endset temperature (K)
T_p	phase change temperature (K)
S_T	source term, dimensionless
V	volume (m^3)
V_f	volume of phase change material (m^3)
V_l	liquid volume of solid–liquid phase (m^3)
ε	carbon foam porosity
δ	liquid fraction in the REV element, dimensionless
ρ_s	phase change material solid density (kg/m^3)
ρ_l	phase change material liquid density (kg/m^3)

Subscripts

f	fluid phase (phase change material)
s	carbon foam solid phase
p_s	carbon foam solid
L	liquid phase
s	solid phase
H	module height

Abbreviations

PCMs	phase change materials
PW	paraffin wax
MWCNTs	Multi Walled Carbon Nano-tubes
CNTs	carbon nanotubes
CF	carbon foam
CFD	computational fluid dynamics
REV	representative elementary volume

et al. [12] presented a numerical study to investigate and assess the heat transfer behavior of a copper and salt composite. A mixture of nitrates, KNO_3–$NaNO_3$, within a deformable spherical shell coating of copper was used as an encapsulated phase change material. The novel copper/salt composite was proven to be an attractive material for heat storage.

On the other hand, porous media has been widely used for thermal management (TM) of many engineering applications especially electronic equipment. The Main advantage of a porous system in such applications is its high surface area-to-volume ratio which leads to enhanced heat transport and miniaturization of thermal systems. Foam material is a highly permeable porous medium characterized by the presence of two or more phases. One of these phases is a solid phase and the other can be fluid or just void spaces. In open cell metal or carbon foams, void spaces are connected to each other leading to a high permeability. Effective thermal conductivity, interfacial surface area, and permeability are the properties that control the performance of thermal management modules and heat sink. Open cell metal foams have appropriate values of these properties which make them highly recommended as a heat sink for thermal management of electronic devices. Weaver and Viskanta [13] performed numerical and experimental investigations for the phase change of water in saturated porous media contained in various enclosures. Solid–liquid interface and fluid motion were observed directly. The effects of natural convection and porous media (spherical glass beads) on the solidification and fluid motion were reported. Beckermann and Viskanta [14] carried out numerical and experimental studies for the solid/liquid phase change in porous media with natural convection in the molten region. Natural convection in the melt as well as heat conduction in the solid is found to considerably influence the interface shape and movement during both melting and solidification process.

The integration of foam structure of high thermal conductivity to accommodate the PCM has received the attention of many researchers due to eliminating the short comings of each of them if it is used individually in thermal management of electronic devices. Mauran et al. [15] used a solid matrix made of graphite as a support structure of low thermal conductivity reactive salts as PCM. Alawadhi and Amon [16] used Aluminum foam as a support structure and Eiconsane as a PCM in conducting experimental and numerical investigation of a TM unit for portable electronic devices. Lafdi et al. [17] conducted an experimental investigation of heat transfer within a composite of PCM infiltrated in high thermal conductivity foam. Aluminum foams with different pore sizes and porosities were used as the porous material and low melting temperature paraffin wax was used as the PCM. Khateeb et al. [18,19] investigated the utilization of aluminum foams filled with paraffin wax as a passive thermal management system for a lithium-ion battery. Hong and Herling [20] analyzed the effects of geometric parameters of foam on the thermal performance of PCM/aluminum foam heat sinks. They concluded that the aluminum foams with larger surface area density utilized more latent heat within a given period of time which helped in improving the thermal performance of the heat sink. Other researchers used porous graphite to improve wax thermal properties [21–24].

Zhou and Zhao [25] presented an experimental study on heat transfer characteristics of PCMs embedded in open cell metal foams and expanded graphite, respectively. In that study the paraffin wax RT27 and calcium chloride hexahydrate are employed as the heat storage media and the transient heat transfer behavior is measured. The results indicated that the addition of porous materials, either open-cell metal foams or expanded graphite, can enhance the heat transfer rate of PCMs. Yang and Garimella [26] investigated the melting of PCMs embedded in metal foams. The two-temperature model developed accounts for volume change in the PCM upon melting. Effects of volume shrinkage/expansion are considered for different interstitial heat transfer rates between the foam and PCM. Zhong et al. [27] used a Mesophase pitch based graphite foams (GFs) with different thermal properties and pore-size to increase the thermal diffusivity of PCM, paraffin wax, for latent heat thermal energy storage application. Their results indicated that thermal diffusivity of the Paraffin-GF can be enhanced 190, 270, 500, and 570 times as compared with that of pure paraffin wax. Latent heat of Paraffin-GF systems increased with the increase of the mass ratio of the paraffin wax in the composite. Zhao et al. [28] experimentally investigated the solid/liquid phase change (melting and solidification) processes of PCM infiltrated in metal foam. Paraffin wax RT58 is used as PCM, in which metal foams are embedded to enhance the heat transfer. PCM composites based on low-density polyethylene (LDPE) with paraffin waxes were investigated in the study of Trigui et al. [29]. The composites were prepared using a melt mixing method with a Brabender-Plastograph. The LDPE as the supporting matrix kept

the molten waxes in compact shape during its phase transition from solid to liquid. The operation and operating parameters of a small-scale Thermal Energy Storage (TES) device that collects and stores heat in a PCM was explored by Thapa et al. [30]. They studied the fabrication and analysis of small-scale TES with conductivity enhancement. Lachheb et al. [31] studied the effect of combining two types of graphite (Synthetic graphite Timrex SFG75 and graphite waste obtained from damaged Tubular graphite Heat Exchangers) with paraffin in an attempt to improve thermal conductivity of paraffin PCM. The results showed that the thermal conductivity and thermal diffusivity are greatly influenced by the graphite addition.

The difference in thermal properties of the foam and the PCM cause a problem which has been defined by some authors as thermal non-equilibrium. The phenomenon of thermal non-equilibrium can be ignored when the thermal properties of the two phases are close to one another. Mesalhy et al. [32] carried out numerical and experimental studies to investigate the thermal characteristics of a cylindrical thermal protection system made of carbon foam matrix saturated with PCM. Their results illustrated that the stability of the thermal performance of composite matrix was dependent on the porosity of the foam and was better for higher porosity foams. Quintard et al. [33] carried out an extensive analysis to determine the conditions for local thermal equilibrium. They concluded that the deviation from local thermal equilibrium would be significant if there is a large difference between the physical properties of the fluid and solid phases. Mesalhy et al. [34] performed a numerical study to analyze the phase change process in a PCM/foam cylindrical composite. They used the volume averaged technique to solve the conservation equations of mass, momentum, and energy with phase change inside the porous matrix. The critical problem of local thermal non-equilibrium was addressed by using separate energy equations for the two phases. Recently, Lafdi et al. [35] proposed a numerical study to investigate and predict the thermal performance of graphite foams infiltrated with PCMs, for space and terrestrial energy storage systems. The numerical model is based on a volume averaging technique while a finite volume method has been used to discretize the heat diffusion equation. They concluded that the PCM–foam system thermal performance has been improved significantly due to the high thermal conductivity of graphite foams.

More recently, the idea of inserting carbon nanotubes, as a thermal enhancer in PCMs was experimentally introduced and tested. Alshaer et al. [36] experimentally studied the effect of inserting carbon nanotubes on the latent heat and thermal conductivities of Paraffin wax, RT65. The results showed a high increase in the composite thermal conductivity achieved by a small amount of nanotubes and the latent heat increased linearly with the amount of nanotubes added. Recently, Raam Dheep and Sreekumar [37] carried out a review to investigate influence of nanomaterials on properties of latent heat solar thermal energy storage materials. More recently Alshaer et al. [38,39] presented experimental and numerical investigation of the effect of insertion of Paraffin Wax RT65 as phase change material and Multi Wall Carbon Nano Tubes (MWCNTs) as thermal conductivity enhancer in carbon foam (CF-20) micro structure modules on the thermal management of electronic devices. Studies were conducted for fixed values of carbon foam porosity, thermal conductivity and PCM thermo physical properties.

The above literature showed that limited numerical investigations were conducted for TM methods using PCMs embedded in carbon foam base structures. Most of the studies were conducted for specific fixed values of the controlled parameters (thermo physical properties of the PCM and carbon foam). The effect of concerned levels of thermal conductivities of carbon foam or PCM (raw or enhanced materials), levels of heat of fusion and fusion temperatures and levels of PCM amounts and corresponding different kinds of porous graphite of different porosities are not investigated in detail. Such investigation needs detailed parametric studies of these controlling parameters. Therefore, the present work aims to perform detailed parametric studies for the performance of a carbon foam base structure module saturated with PCMs for thermal management of electronic equipment. Different carbon foam structures having different porosities, different conductivities, PCMs of different thermal conductivities, fusion temperature, and fusion heat, module geometrical parameters and module power densities are parametrically studied.

2. Physical model and studied parameters

2.1. Physical model

Fig. 1 shows the physical model suggested for the parametric study of the characteristics of thermal management of the composite module. The base structure of the module is carbon foam imbedded with PCM. The module is considered to be heated from bottom side with a constant heat flux condition. To maintain an effective cooling of the module, the boundary condition of the top side is approximated and selected to be a constant temperature equal to the initial temperature of the system. The right and left sides of the module are considered adiabatic.

2.2. Ranges of studied parameters and base line case

The parametric study includes studying the effect of the following parameters on the performance of the thermal management modules within the given ranges:

- Porosity (ε) of the carbon foam base structure in the range from 0.6 to 0.85.
- Carbon foam skeleton thermal conductivity in the range from 26 to 400 W/m K.
- Heat of fusion of the PCM in the range from 160 kJ/kg to 350 kJ/kg.
- PCM fusion temperature from 50 °C to 70 °C
- Module height range from 30 to 50 mm for a fixed base dimension of 50 × 50 mm.
- Input heat flux in the range from 12,000 to 96,000 W/m^2.
- PCMs thermal conductivity from 0.22 W/m K to 0.4 W/m K.

The ranges of the thermo-physical properties of the PCMs were chosen to cover the wide ranges of the PCMs properties available in the market and used in the different engineering applications such

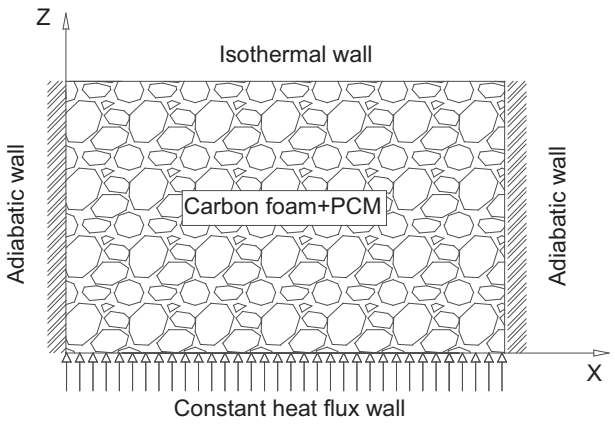

Fig. 1. Schematic diagram for physical model.

as different types of paraffin wax (RT16, RT27, RT56, RT58, RT65), Eiconsane, reactive salts, calcium chloride hexahydrate, etc).

A reference set of parameters values (CF porosity = 0.85, CF skeleton thermal conductivity = 26 W/m K, PCM latent heat of fusion = 160 kJ/kg, PCM fusion temperature = 65 °C, PCMs thermal conductivity = 0.22 W/m K. module height = 40 mm and module power density = 12,000 W/m^2) has been selected to represent a base line case. The effects of variation of CF porosity, CF skeleton thermal conductivity, PCM latent heat of fusion, PCM fusion temperature, module height and module power density have been investigated by changing one single parameter at a time. Sometimes more variables may be changed at a time to clearly demonstrate a certain phenomena.

3. Numerical techniques

The volume averaged energy equation is used to model the heat transfer process inside the porous composite with and without PCM. Considering a representative elementary volume (REV) undergoing phase change process in a porous media as shown in Fig. 2. The REV of volume "V" contains the carbon foam solid phase "s". The porous pores of carbon foam of porosity "ε" are filled with phase change material with volume "V_f".

In the present analysis, the properties of each phase are assumed isotropic and constant. When the solid–liquid phase change process takes place, the liquid fraction in the fluid phase is defined as:

$$g_l = \frac{V_l}{V_f} \tag{1}$$

where V_l is the liquid volume in the fluid phase.

The liquid fraction "δ " in the REV element is defined as:

$$\delta = \varepsilon g_l \tag{2}$$

where $\varepsilon = \frac{V_f}{V}$ is the carbon foam porosity.

It should be mentioned that there are two solid phases inside the REV. The PCM solid referred by the subscript "s" and the carbon foam solid referred by the subscript "ps". Due to the small size of the carbon foam pores, which is ranging between 200 and 800 μm, it is assumed that the convection motion of the molten liquid phase is negligible. This assumption is supported by [22,27] where the convection motion is neglected due to the small size of the pores. Also the assumption of neglecting the convection motion liquid phase is supported by the findings of [35] who examined the role of natural convection within the pores by discretizing and solving the continuity and momentum equations numerically over the fluid domain. They found that the role of natural convection within the pores turned out to be negligible due to the small values of the pore diameter and temperature difference (the Grashof and Rayleigh numbers based on the pore diameter are of the order of 1 and 10, respectively).

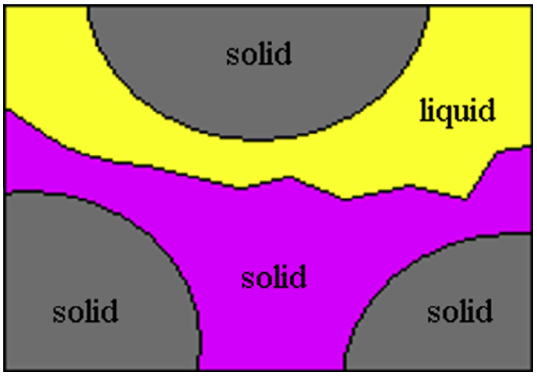

Fig. 2. Representative elementary volume for phase change in a porous media.

Assuming thermodynamic equilibrium between the solid (s and ps) and liquid (l) phases, the volume averaged energy equation for the porous matrix (ps)/solid (s)/liquid (l) can be written as

$$\frac{\partial}{\partial t}\left[\varepsilon(g_l\rho_l h_l + (1-g_l)\rho_s h_s) + (1-\varepsilon)\rho_{ps}h_{ps}\right] = \nabla\cdot(k_{eff}\nabla T) + S_T \tag{3}$$

where k_{eff} is the effective thermal conductivity and S_T accounts for other source terms. For a volume element undergoing phase change (i.e. for $0 < g_l < 1$), a change in the main enthalpy of the fluid is due to a change in the sensible heat of the liquid/solid mixture plus contribution of the latent heat. To a good approximation, this can be expressed as:

$$d((g_l\rho_l h_l + (1-g_l)\rho_s h_s) = (g_l(\rho c_p)_l + (1-g_l)(\rho c_p)_s)dT + \rho_l L dg_l \tag{4}$$

where L is the latent heat of phase change. The liquid phase enthalpy is given by:

$$h_l = (c_p)_l T + L \tag{5}$$

Substituting Eqs. (5) into (3) results in:

$$\frac{\partial(\overline{\rho c_p})T}{\partial t} = \nabla\cdot(k_{eff}\nabla T) - \varepsilon\rho L\frac{\partial g_l}{\partial t} + S_T \tag{6}$$

where

$$k_{eff} = (1-\varepsilon)k_{ps} + \varepsilon(g_l k_l + (1-g_l)k_s) \tag{7}$$

and:

$$\overline{\rho c_p} = (1-\varepsilon)(\rho c_p)_{ps} + \varepsilon[g_l(\rho c_p)_l + (1-g_l)(\rho c_p)_s] \tag{8}$$

Eq. (6) is applicable to the whole domain by proper assignment of thermo-physical properties, porosity, solid and fluid phases. The governing equation) Eq. (6) contains an extra unknown "g_l" which is function of the temperature. Iterations for g_l are obtained as follows:

$$g_l^{i+1} = g_l^i + corr \tag{9}$$

where i refer to the iteration number and $corr$ is the correction term given by:

$$corr = \frac{c_p\left(T^i - T_p\right)}{L} \tag{10}$$

where T_p is the phase change temperature. At convergence $T^i = T_p$ and $corr = 0$.

For phase change materials undergoing phase change at a given constant phase change temperature, T_p is a constant value independent of liquid fraction g_l.

In the present PCM undergoes solid/liquid phase change over a temperature range between T_{onset} and T_{endset}, a linear variation of T_p is assumed as follows:

$$T_p = T_{onset} + g_l(T_{endset} - T_{onset}) \tag{11}$$

the heat equations for wall aluminum enclosure and the insulation can be written as:

$$\frac{\partial^2 T}{\partial^2 x} = \frac{\rho c}{k}\frac{\partial T}{\partial t} \tag{12}$$

where x is the direction normal to the heat transfer.

The above system of equations is subject to the following boundary and initial conditions as shown in Fig. 1

– Constant heat flux applied at the bottom of the system.
– Top wall temperature is constant and equal to the initial temperature of the system.
– Initial temperature of the system = 25 °C.
– Adiabatic side walls.

The above system of equations have been solved using a Thétis CFD code [40]. Thétis employs a finite volume discretization of the governing equations. The discretized equations are solved using iterations at a given time step and considered converged when the residual is less than 10^{-15}. Internal iterations for liquid fraction are considered converged when corr $\leqslant 10^{-6}$. A time step of 1 s has been implemented in all simulations. The system boundary conditions have been stated in Section 2.2 with system initial temperature of 25 °C. All CFs used in the present study have a fixed skeleton density of 2200 kg/m^3 and a specific heat of 750 J/g K. All PCMs used have a fixed conductivity value of 0.22 W/m K.

4. Grid independent study and code validation

The grid generation for whole domain of the physical model described in Fig. 1 is shown in Fig. 3. A grid sensitivity analysis has been performed on the base line case to reach the proper grid size for grid independent results. Table 1 shows the steady state temperature of the module bottom heated surface at different values of grid sizes and 1 s time step for modules with and without PCM for the structures and properties of the base line case. Different time steps values of 1, 0.1 and 0.01 s, have been implemented in the study. It has been observed that there is no discrepancy between the numerical values of Table 1 at the different time steps. This is attributed to the implicit nature of the energy equation and the absence of advection terms.

As shown in the table the temperature history becomes constant within an error of 0.001 °C for grid size of 300 × 300 and more. Therefore a time step of 1 s. and a grid size of 300 × 300 have been implemented in all simulations in order to reduce the computer run time.

Validations of the present mathematical model have been carried out by comparing code prediction of modules surface temperature with previous experimental results. Fig. 4 shows the comparison of code predictions with experimental data of Alshaer et al. [38] obtained for pure CF-20 module and CF-20/RT65 modules having same thermo physical properties, physical dimensions and boundary conditions. The error bars of the experimental work of Alshaer et al. [38] was 0.3 °C (±0.15 °C uncertainty). As shown in the figure, the model perfectly predicts

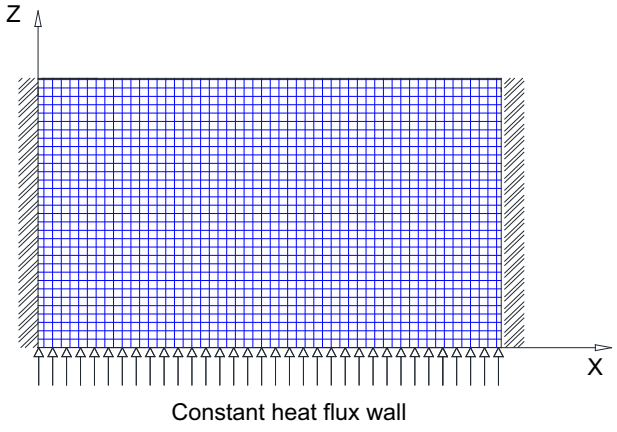

Fig. 3. Grid shape.

Table 1
Steady state temperature values for different grid sizes of CF and CF/PCM sample modules at base line case.

Grid size	*T*, °C, for CF	*T*, °C, for CF + PCM
50 × 50	148.05	143.10
100 × 100	148.11	143.20
200 × 200	148.20	143.28
300 × 300	148.23	143.30
400 × 400	148.24	143.30

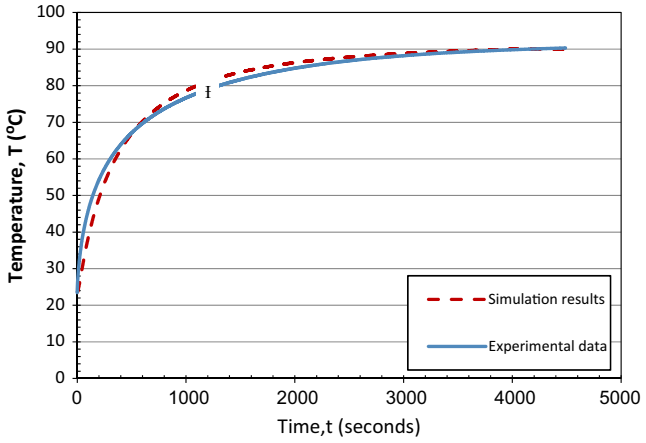

(a) pure CF module.

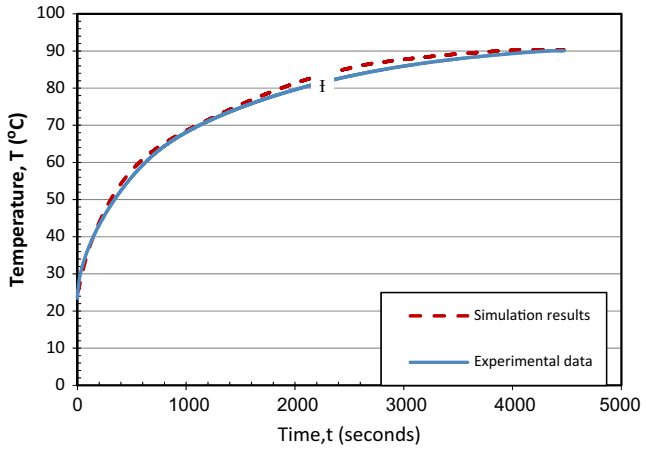

(b) CF/RT65 module

Fig. 4. Code validation by comparing code predictions for modules base temperature with previous experimental data of Alshaer et al. [38] (error bars: = 0.3 °C).

the experimental results. The maximum deviation between the model prediction and the experimental results of Alshaer et al. [38] during the entire time history was about 1.95 °C (including 0.15 °C uncertainty) which represent about 2.1% of the module temperature.

5. Results and discussion

Numerical experiments have been carried out for different values of CF porosity = (0.6, 0.7, 0.8 and 0.85), CF skeleton thermal conductivity = (26, 50, 100, 200, 400 W/m K), PCM latent heat of fusion = (160, 250, 350 kJ/kg) , PCM fusion temperature = (50, 65, 70 °C), module height = (30, 40, 50 mm) and power density = (12,000, 24,000, 48,000, 96,000 W/m^2). Firstly the temperature isotherm, melting front and the effect of insertion of PCM

are discussed for the base line case, then the effects of variation of CF porosity, CF skeleton thermal conductivity, PCM latent heat of fusion, PCM fusion temperature, module height and module power density have been investigated by changing one single parameter of the base line case at a time. Sometimes more variables may be changed at a time to clearly demonstrate a certain phenomenon.

5.1. Temperature isotherm, melting front and effect of PCM insertion

Fig. 5 shows the temperature isotherms distributions inside CF/PCM composite module at the base line conditions during the first 3000 s in a time step of 500 s. The temperature history of the base of the CF/PCM module at the base line conditions (Picked up from Fig. 5) compared to the ones of the pure CF module is shown in Fig. 6. The figure shows that: (i) for pure carbon foam, the steady state temperature has been reached quickly during the first 200 s, (ii) the insertion of the PCM in the module delay the occurrence of the steady state temperature by 1500 s, (iii) insertion of the PCM in the carbon foam dramatically reduces the transient temperature level of the module base and reduces the steady state temperature of the module base by 3 °C. The dramatic reduction in the transient temperature level of the module base due to the insertion of the PCM can be attributed to the absorbed energy in melting of the PCM inside the module. The time lag in reaching the steady state temperature and the reduction in steady state

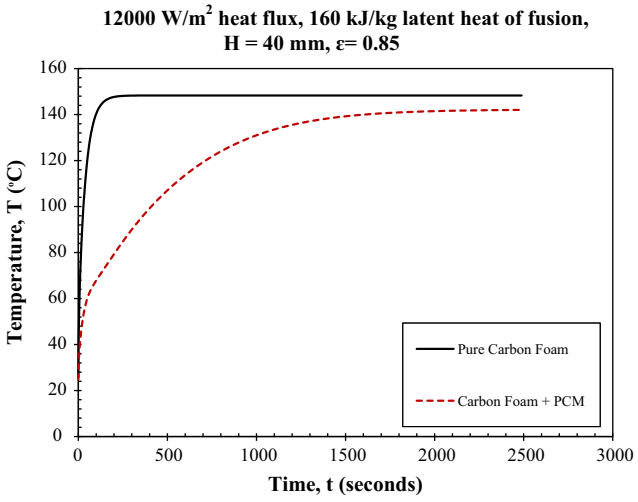

Fig. 6. Comparison between temperatures histories of CF and CF/PCM at base line case.

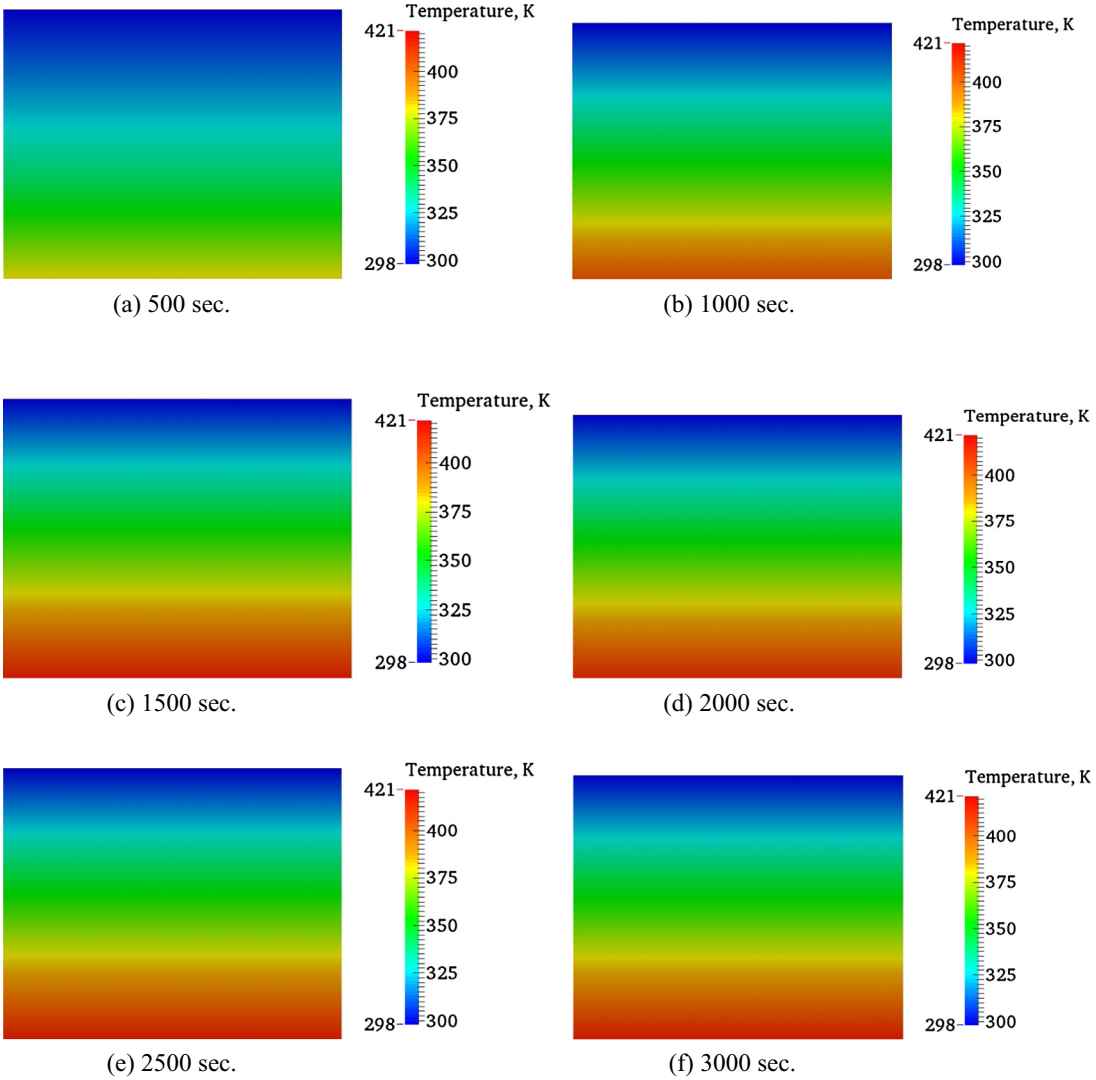

Fig. 5. Temperature distribution at different times for CF/PCM module at base line case.

temperature due to insertion of PCM can be attributed to the combined effect of the increase of the structure effective volumetric specific heat due to the presence of PCM and the absorbed energy in melting of the PCM inside the module. The dramatic reduction of the transient temperature level and the time lag and reduction in the steady state temperature due to the insertion of the PCM enhances the cooling of the electronic equipment especially in the cyclic modes of operation [38].

The solid fraction distribution during PCM melting inside CF/PCM composite module during the first 3000 s are presented in Fig. 7 in a time step of 500 s. Fig. 7 shows that PCM melting process passes by three regions: solid, mush, and pure liquid. Starting at time $t = 0$, the temperature of active domain is held below the freezing temperature of PCM (65 °C) where the temperature is 25 °C. The temperature of the module bottom wall is still below the melting temperature of the PCM until reaching a time of about 100 s, after then the PCM at the module bottom starts melting and the solid melting front travels toward the top of the module with time. Colorized contours of the volume fraction of the PCM during melting at various time intervals have been shown in Fig. 7. It should be mentioned that the color red is used to identify the liquid phase, whereas color blue is indicative of the frozen solid phase and in between is the mushy zone.

5.2. Effect of carbon foam porosity

The effect of carbon foam porosity on the thermal behavior of the modules are shown in Figs. 8 and 9 for pure carbon foam and carbon foam saturated with PCM, respectively. Both figures show the increase of the module surface temperature with the increase of carbon foam porosity. This can be attributed to the decrease of the effective thermal conductivity of the carbon foam with the increase of the porosity due to the bad thermal conductivity of the air or PCM (porosity filling material) as compared to the skeleton thermal conductivity of the carbon ligament. Decreasing the effective thermal conductivity decreases heat transfer rate which results in increasing module surface temperature. Fig. 9 shows that in the first time interval ($t < 100$) the rate of module base temperature rise is very high after then ($t > 100$) the rate of temperature rise slow down. This can be attributed to that in the first time interval ($t < 100$) the module temperature is still lower than the fusion temperature of the PCM (65 °C) and the fusion of the PCM is not started yet, after then ($t > 100$ s) the PCM starts to melt and most of the released heat is utilized in the phase change process and consequently reducing the heat responsible on module temperature rise leading to slower module temperature rise.

Fig. 9 also shows that, increasing the porosity of CF/PCM module decreases the delays the time at which the module approaching steady state temperature. This can be attributed to the increase of the amount of PCM in the module with increasing the porosity and this increases the heat utilized in the PCM phase change material and consequently reducing heat responsible on module temperature rise which leads to slower module temperature rise and delaying the approaching the steady state temperature.

5.3. Effect of module height

Fig. 10 shows module temperature histories for different module heights. As shown in the figure increasing the module height increases the module base temperature. This can be attributed to the increase of module thermal resistance which leads to lower heat transfer rate and consequently higher temperature level at the module base. On the other hand, Fig. 10 shows that increasing module height increases the time of approaching steady state temperature. This can be attributed to the increase of the amount of PCM inside the module with increasing the thickness. Increasing the PCM amounts consumes more heat in its melting and consequently reduces the remaining heat that causes module temperature rise and this increase the time necessary to approach steady state temperature.

5.4. Effect of PCM fusion temperature

Fig. 11 shows the temperature history of the base of CF/PCM modules using different PCMs of different fusion temperatures. As shown in the figure, the module fusion temperature does not have an effect on the steady state temperature however decreasing PCM fusion temperature slightly decreases the module temperature in the transient interval. This can be attributed to the early starting of the PCM melting for lower fusion temperature which leads to lower module temperature.

5.5. Effect of PCM heat of fusion

Fig. 12 shows the effect of the latent heat of fusion of the PCM on the temperature history of the CF/PCM modules. As shown in the figure, increasing the heat of fusion decreases the module temperature in the transient interval and increases the time of approaching the steady state temperature. This can be attributed to the consuming of most of the heat released in melting of the PCM and reducing the remaining heat which is responsible on the temperature rise of the module. Fig. 12 also shows the independence of the value of the steady state temperature on the latent heat of fusion.

Figs. 11 and 12 concludes that using PCM of high latent heat of fusion and low fusion temperature dramatically decrease transient temperature and increase the time needed to approach steady state temperature. This conclude that using PCM of high latent heat and relatively low fusion temperature in CF/PCM thermal management modules has efficient performance especially in cyclic power operation where the modules are always operated in the transient period.

5.6. Effect of carbon foam and PCM thermal conductivities

It is well known from heat transfer basics that increasing the effective thermal conductivity of the CF/PCM module by increasing carbon foam skeleton thermal conductivity leads to higher heat transfer rate inside the module and consequently lower temperature of the module base. For example, Fig. 13 shows that for the same power density 1200 W/m^2, increasing thermal conductivity from 26 to 50 W/m k dramatically decreases the module transient and steady state temperatures and the time of approaching the steady state temperature. This concludes that CF/PCM modules of higher CF skeleton thermal conductivities can withstand high power densities and keep the module within the safe operation temperatures (Less than 88 °C). Fig. 13 Shows the temperature histories of the modules base using different CF skeleton thermal conductivities and subjected to different power densities. As shown in the figure, the power densities that the module can withstand is doubled by doubling the CF skeleton thermal conductivities. The figure also shows that increasing power densities accelerate the approaching of steady state temperature and this can be attributed to the fast melting of the PCM inside the module due to the high power density. The figure also shows the decrease of the module temperature in the transient part with the decrease of the thermal conductivity (for the same value of power density/thermal conductivity ratio). This can be attributed to the decrease of heat diffusion rate in the module and this means more utilization of the heat in melting the PCM leading to low temperatures.

Fig. 14 shows the effect of PCM thermal conductivity on the temperature histories of the module base. As shown in the figure

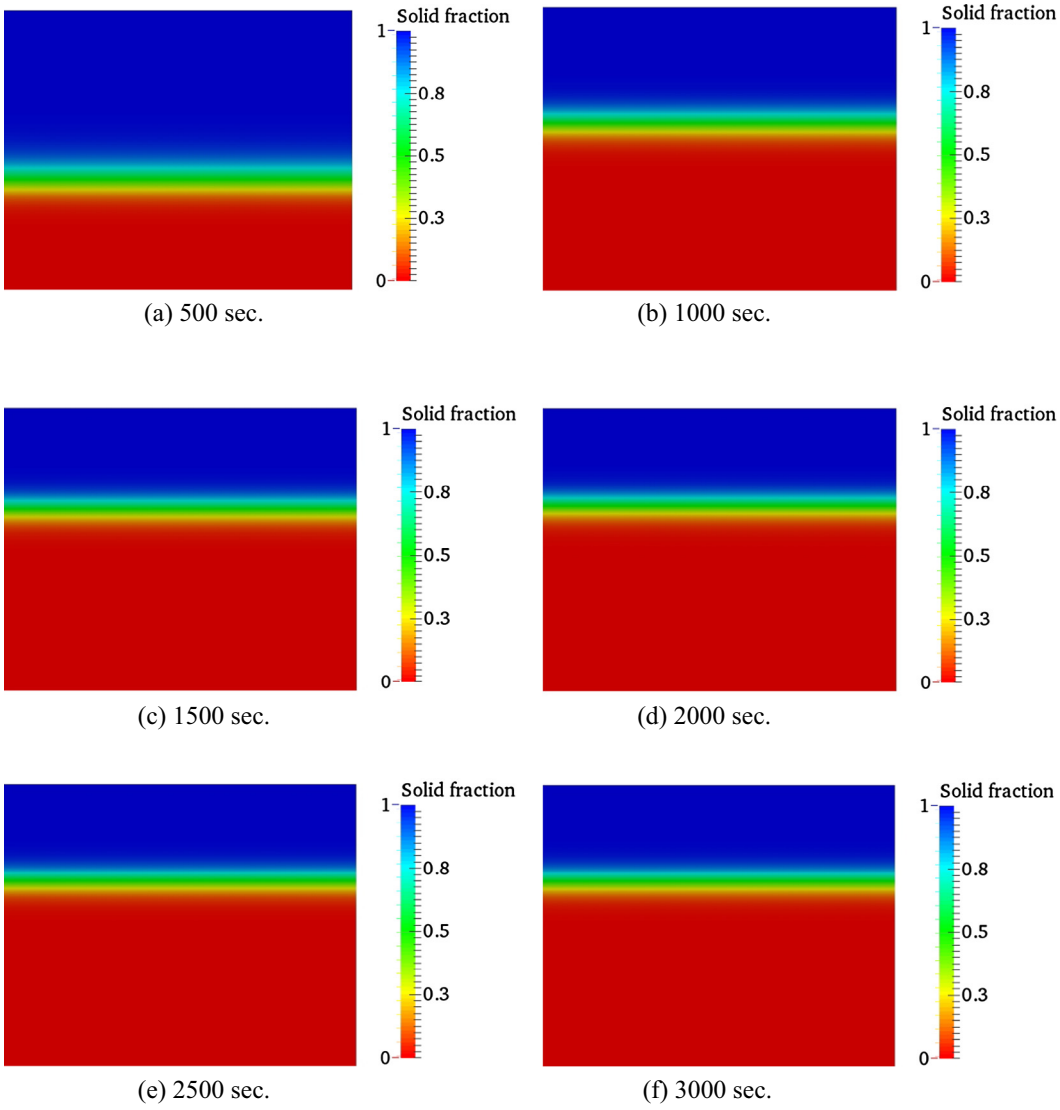

Fig. 7. Solid fraction versus time for CF/PCM module at base line case.

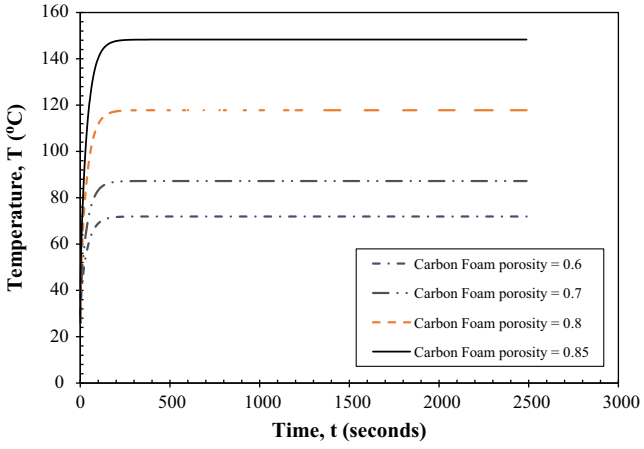

Fig. 8. Temperature history for pure CF module base at different porosities (other properties are same of base line case).

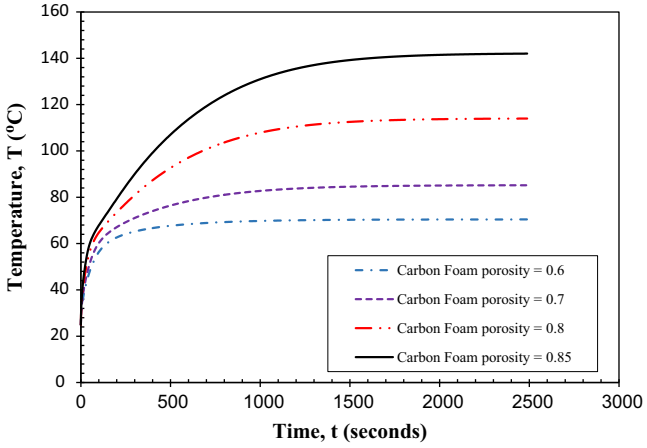

Fig. 9. Temperature history of CF/PCM module base at different porosities (other properties are same of base line case).

the module temperature relatively decreases with the increase of thermal conductivity of the PCM. This can be attributed to the increase of the effective thermal conductivity of the module by increasing the PCM thermal conductivity and that lead to higher heat transfer rate and lower module temperature. The results show that the effect of PCM thermal conductivity becomes less dominant at smaller carbon foam porosities.

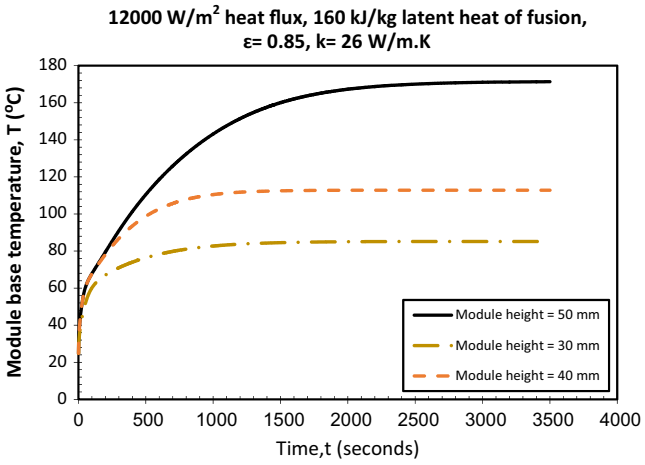

Fig. 10. Temperature history of CF/PCM module base at different module heights (other properties are same of base line case).

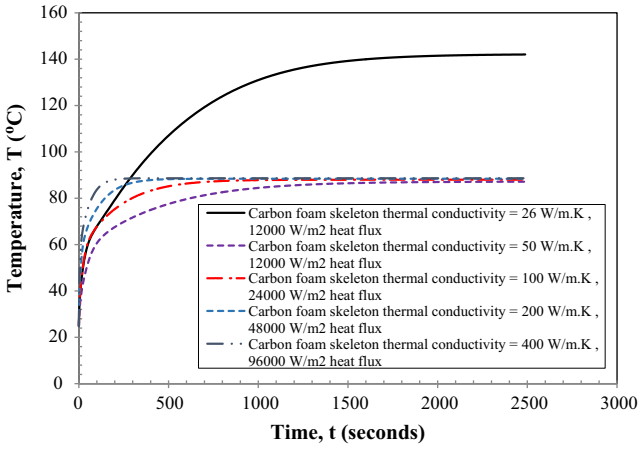

Fig. 13. Temperature history of CF/PCM module base at different CF skeleton thermal conductivity and applied heat flux levels (other properties are same of base line case).

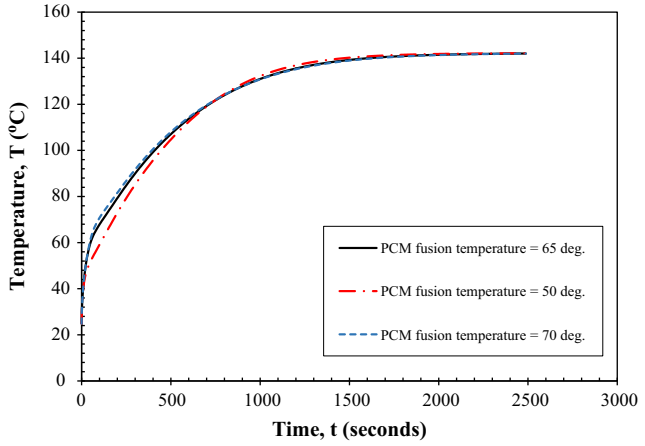

Fig. 11. Temperature history comparison of CF/PCM module base at different PCM fusion temperatures (other properties are same of base line case).

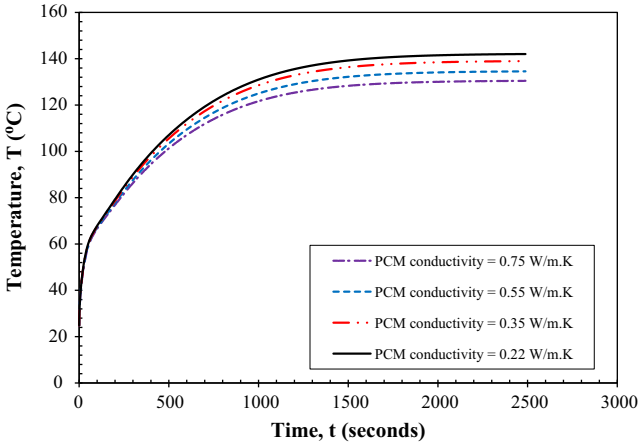

Fig. 14. Effect of PCM thermal conductivity on temperature history of CF/PCM module base (other properties are same of base line case).

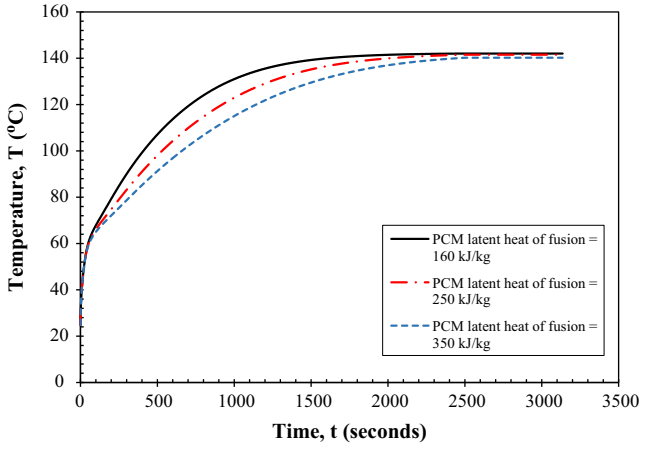

Fig. 12. Temperature history of CF/PCM module base at different PCM latent heat of fusion (other properties are same of base line case).

Comparing Figs. 13 and 14 show that the effect of carbon foam skeleton thermal conductivity is more dominant than the effect of PCM thermal conductivity. For example increasing the thermal conductivity of the PCM by 50% decreases the steady state temperature of the module base by 1.6% (2 °C) however increasing the skeleton thermal conductivity of the carbon foam by 50% (from 26 to 50 W/m k)decreases the steady state temperature by 43% (from 141 to 82 °C).

5.7. Guidelines for CF/PCM thermo physical parameters selections

For thermal management modules operating under cyclic power and repetitively on–off operations, the modules will operate all the time in the transient temperature intervals shown in Figs. 5–14. In this case, the target in module selection is to have lower transient temperature and based on the present results this can be obtained using carbon foam of high porosity, PCM of high heat of fusion and low temperature of fusion and module of relatively high thickness. The skeleton thermal conductivity of the carbon foam should be relatively low but not lower than the value that overheat the module temperature above the safe limits.

For modules that operate continuously at a uniform power density, the modules will operate most of the time at steady state temperatures that are shown in Figs. 5–14. The target of the module selection in this situation is to have low steady state temperature providing that the transient temperature is lower than the steady state value and based on the present results this

can be obtained by using modules of high skeleton thermal conductivity and low porosity and PCM of high heat of fusion and high thermal conductivity.

6. Conclusion

Detailed numerical parametric studies of CF/PCM modules for thermal management systems using carbon foams of different porosities structures and different skeleton thermal conductivities saturated with different PCMs having different thermal conductivities, heat of fusions and fusion temperatures. The effects of module thickness and level of power densities are also investigated. The results show: (i) the increase of the module temperature with the increase of the carbon foam porosity, however increasing the porosity decreases the rate of module temperature rise and consequently delays the time of approaching steady state temperature, (ii) the increase of the module temperature with increasing the module height however increasing module height increases the time of approaching steady state temperature, (iii) the module fusion temperature does not have an effect on the steady state temperature, however decreasing PCM fusion temperature slightly decreases the module temperature in the transient interval, (iv) the decrease of the transient module temperature and the increase of the time of approaching steady state temperature with increasing the heat of fusion, and (v) the power densities that the module can withstand is doubled by doubling the CF skeleton thermal conductivities, however increasing power densities accelerate the approaching of steady state temperature and decreasing the thermal conductivity decreases the module temperature in the transient interval. Guidelines for selecting carbon foam structure and PCM combination for different module power densities were proposed.

References

[1] Farid MM, Khudhair AM, Razack SAK, Al-Hallaj S. A review on phase change energy storage: materials and applications. Energy Conver Manage 2004;45:1597–615.
[2] Verma P, Varun, Singhal SK. Review of mathematical modeling on latent heat thermal energy storage systems using phase-change material. Renew Sustain Energy Rev 2008;12:999–1031.
[3] Agyenim F, Hewitt N, Eames P, Smyth M. A review of materials, heat transfer and phase change problem formulation for latent heat thermal energy storage systems. Renew Sustain Energy Rev 2010;14:615–28.
[4] Sharma SD, Sagara K. Latent heat storage materials and systems: a review. Int. J. Green Energy 2005;2:1–56.
[5] Zalba B, Marin JM, Cabeza LF, Mehling H. Review on thermal energy storage with phase change: materials, heat transfer analysis and applications. Appl Therm Eng 2003;23:251–83.
[6] Kenisarin M, Mahkamov K. Solar energy storage using phase change materials. Renew Sustain Energy Rev 2007;11:1913–65.
[7] Mallik Sabuj, Ekere Ndy, Best Chris, Bhatti Raj. Investigation of thermal management materials for automotive electronic. Appl Therm Eng 2011;31:355–62.
[8] Hussein HMS, El-Ghetany HH, Nada SA. Experimental investigation of a novel indirect solar cooker with an indoor PCM thermal storage and cooking unit. Energy Convers Manage 2008;49:2237–46.
[9] Wang Yi-Hsien, Yang Yue-Tzu. Three-dimensional transient cooling simulations of a portable electronic device using PCM (phase change materials) in multi-fin heat sink. Energy 2011;36:5214–24.
[10] Hoogendoorn CJ, Bart GC. Performance and modeling of latent heat storage. Sol Energy 1992;98:53–8.
[11] Zhang H, Baeyens J, Degrève Jan, Cáceres G, Segal Ricardo, Pitié F. Latent heat storage with tubular-encapsulated phase change materials (PCMs). Energy 2014;76:66–72.
[12] Parrado C, Cáceres G, Bize F, Bubnovich V, Baeyens J, Degrève J, et al. Thermo-mechanical analysis of copper-encapsulated NaNO3–KNO3. Chem Eng Res Des 2015;93:224–31.
[13] Weaver JA, Viskanta R. Freezing of water saturated porous media in a rectangular cavity. Int Commun Heat Mass Trans 1986;13:245–52.
[14] Beckermann C, Viskanta R. Natural convection solid/liquid phase change in porous media. Int J Heat Mass Trans 1988;31:35–46.
[15] Mauran S, Prades P, L'haridon F. Heat and mass transfer in consolidated reacting beds for thermochemical systems. Heat Recov Syst CHP 1993;4:315–9.
[16] Alawadhi EM, Amon CH. Performance analysis of an enhanced PCM thermal control unit. Proc ITherm 2000:283–9.
[17] Lafdi K, Mesalhy O, Shaikh S. Experimental study on the influence of foam porosity and pore size on the melting of phase change materials. J Appl Phys 2007;1–2:083549–55.
[18] Khateeb SA, Farid MM, Selman JR, Al-Hallaj S. Design and simulation of a lithium-ion battery with a phase change material thermal management system for an electric scooter. J Power Sources 2004;128:292–307.
[19] Khateeb SA, Amiruddin S, Farid MM, Selman JR, Al-Hallaj S. Thermal management of Li-ion battery with phase change material for electric scooters: experimental validation. J Power Sources 2005;142:345–53.
[20] Hong S, Herling DR. Open-cell aluminum foams filled with phase change materials as compact heat sinks. Scripta Mater 2006;55:887–90.
[21] Py X, Olives R, Mauran S. Paraffin/porous-graphite-matrix composites as a high and constant power thermal storage material. Int J Heat Mass Trans 2001;44:2727–37.
[22] Mills A, Farid M, Selman JR, Al-Hallaj S. Thermal conductivity enhancement of phase change materials using a graphite matrix. J Appl Therm Eng 2006;66:1652–61.
[23] Zhang Z, Fang X. Study on paraffin/expanded graphite composite phase change thermal energy storage material. Energy Convers Manage 2005;47:303–10.
[24] Sari A. Form-stable paraffin/high density polyethylene composites as solid–liquid phase change material for thermal energy storage: preparation and thermal properties. Energy Convers Manage 2004;45:2033–42.
[25] Zhou D, Zhao CY. Experimental investigations on heat transfer in phase change materials (PCMs) embedded in porous materials. Appl Therm Eng 2010:1–8.
[26] Yang Z, Garimella SV. Melting of phase change materials with volume change in metal foams. J Heat Trans 2010;132.
[27] Zhong Yajuan, Guo Quangui, Li Sizhong, Shi Jingli, Liu Lang. Heat transfer enhancement of paraffin wax using graphite foam for thermal energy storage. Sol Energy Mater Sol Cells 2010;94:1011–4.
[28] Zhao CY, Lu W, Tian Y. Heat transfer enhancement for thermal energy storage using metal foams embedded within phase change materials (PCMs). Sol Energy 2010;84:1402–12.
[29] Trigui Abdelwaheb, Karkri Mustapha, Krupa Igor. Thermal conductivity and latent heat thermal energy storage properties of LDPE/wax as a shape-stabilized composite phase change material. Energy Convers Manage 2014;77:586–96.
[30] Thapa Suvhashis, Chukwu Sam, Khaliq Abdul, Weiss Leland. Fabrication and analysis of small-scale thermal energy storage with conductivity enhancement. Energy Convers Manage 2014;79:161–70.
[31] Lachheb Mohamed, Karkri Mustapha, Albouchi Fethi, Mzali Foued, Ben Nasrallah Sassi. Thermophysical properties estimation of paraffin/graphite composite phase change material using an inverse method. Energy Convers Manage 2014;82:229–37.
[32] Mesalhy O, Lafdi K, Elgafy A. Carbon foam matrices saturated with PCM for thermal protection purposes. Carbon 2006;44:2080–8.
[33] Quintard M, Whitaker S. One and two equation models in two phase systems. Adv Heat Trans 1993;32:369–464.
[34] Mesalhy O, Lafdi K, Elgafy A, Bowman K. Numerical study for enhancing the thermal conductivity of phase change material (PCM) storage using high thermal conductivity porous matrix. Energy Convers Manage 2005;46:847–67.
[35] Lafdi K, Mesalhy O, Elgafy A. Graphite foams infiltrated with phase change materials as alternative materials for space and terrestrial thermal energy storage applications. Carbon 2008;46:159–68.
[36] Alshaer WG, Palomo del Barrio E, Rady MA, Abdellatif OE, Nada SA. Analysis of the anomalous thermal properties of phase change materials based on paraffin wax and multi walls carbon nanotubes. Int J Heat Mass Trans – Theor Appl 2013;1:297–307.
[37] Raam Dheep G, Sreekumar A. Influence of nanomaterials on properties of latent heat solar thermal energy storage materials – a review. Energy Convers Manage 2014;83:133–48.
[38] Alshaer WG, Nada SA, Rady MA, Palomo del Barrio E, Sommier Alain. Thermal management of electronic devices using carbon foam and PCM/nano-composite. International. J Therm Sci 2015;89:79–86.
[39] Alshaer WG, Nada SA, Rady MA, Cedric Le Bot, Palomo del Barrio E. Numerical investigations of using carbon foam/PCM/Nano carbon tubes composites in thermal management of electronic equipment. Energy Convers Manage 2015;89:873–84.
[40] Thétis, Code de mecanique, http://thetis.enscbp.fr; Jan 2015.